LAPPED DIRECTIONAL TRANSFORM: A NEW TRANSFORM FOR SPECTRAL IMAGE ANALYSIS

Dietmar Kunz

Philips Research Laboratories,
Weisshausstr. 2, D-52066 Aachen,
Germany

Til Aach

Institute for Signal Processing,
Medical University of Luebeck,
Ratzeburger Allee 160, D-23538 Luebeck
aach@informatik.mu-luebeck.de

ABSTRACT

We propose a new real-valued lapped transform for 2D-signal and image processing. Lapped transforms are particularly useful in block-based processing, since their intrinsically overlapping basis functions reduce or prevent block artifacts. Our transform is derived from the modulated lapped transform (MLT), which, as a real-valued and separable transform like the Discrete Cosine Transform, does not allow to unambiguously identify oriented structures from modulus spectra. This is in marked contrast to the (complex-valued) Discrete Fourier Transform (DFT). The new lapped transform is real-valued, and at the same time allows unambiguous detection of spatial orientation. Furthermore, a fast algorithm for this transform exists. As an application example, we investigate the transform's performance in spectral approaches to image restoration and enhancement in comparison to the DFT.

1. INTRODUCTION

Calculation of block or short space spectra from images and image reconstruction from processed block spectra are standard operations in many image processing tasks. Examples are image compression [1] and noise reduction by spectral amplitude estimation [2, 3]. These methods rely on the ability of the spectral transform to concentrate signal energy into only a few coefficients. As shown in [4] for the example of image restoration and enhancement, the performance of block spectra-based algorithms can be considerably improved if perceptually important information, like oriented lines and edges, can be detected and processed in a special manner. In this respect the Discrete Fourier Transform (DFT) is particularly advantageous since the presence of local orientation within a block results in concentration of spectral energy along the line perpendicular to spatial orientation and passing through the origin [4, 5]. The downside, however, of the DFT is that in order to avoid spurious high frequency artifacts, each block must be windowed prior to the transform. The reconstruction property then requires overlapping blocks [6], usually by half the block size in each dimension [2]. Each pixel is hence part of four blocks, resulting in a fourfold increased data volume.

Unlike the DFT, the Discrete Cosine Transform (DCT) does not require windowing, and hence avoids the necessity of overlapping blocks and redundancy. Artifacts at block boundaries may, however, occur. These, in turn, can be prevented by so-called lapped transforms like the Lapped Orthogonal Transform (LOT) [7] or the Modulated Lapped Transform (MLT) [8]. Essentially, these real-valued transforms yield a non-redundant image representation based on overlapping basis functions, thus making these transforms particularly attractive for compression [9].

The discussed real-valued transforms do not, however, allow unambiguous detection of oriented structures from spectral energy concentration. The reason for this is that the DCT is derived as the Fourier transform of vertically and horizontally mirrored blocks. On the one hand, this avoids the spurious high frequency artifacts of the DFT. On the other hand, mirrored orientations are generated. Conversely, this means that a certain spatial orientation cannot be distinguished from its mirrored counterpart when looking at spectral energy concentration. A similar relationship holds for the MLT.

A lapped transform allowing unambiguous detection of spatial orientation from modulus spectra is the complex-valued transform in [10]. Like the DFT with half overlapping blocks, it also results in a fourfold increased data volume.

In the following, we derive a new real-valued lapped transform which permits unambiguous orientation detection. The central idea is to perform two MLTs with different but in some sense complementary basis functions, and to combine the resulting spectra. The transform results in a twofold increased data volume, and is hence "less redundant" than the DFT and the mentioned complex lapped transform [10].

This work was performed while both authors were with Philips Research, Aachen.

2. LAPPED DIRECTIONAL TRANSFORM (LDT)

To derive our new transform — named the Lapped Directional Transform (LDT) — we start with a 1D MLT, which decomposes a 1D signal into overlapping blocks of length $2M$ [8]. The overlap between adjacent blocks is M so that each sample belongs to two blocks.

Let $x_r,\ r = 0, \ldots, 2M-1$ denote the $2M$ samples in a block. The M real-valued basis functions are formed by (co-)sine waves being symmetric around $(M-1)/2$ and anti-symmetric around $(3M-1)/2$ [8]. These functions are modulated by a sine-shaped window function with period $4M$ which is symmetric around the block centre $(2M-1)/2$. Hence, there are only M different basis functions satisfying both symmetry constraints. The transform can be described by a $(M, 2M)$-matrix with entries [8]

$$\begin{aligned} m_{kr} &= \cos\left[\frac{\pi}{2M}\left(r - M + \frac{1}{2}\right)\right] \cdot \\ &\quad \cdot \cos\left[\frac{\pi}{M}\left(r - \frac{M-1}{2}\right)\left(k + \frac{1}{2}\right)\right], \\ &\quad k = 0, \ldots, M-1,\ r = 0, \ldots, 2M-1. \end{aligned} \tag{1}$$

Note that with this definition, there is a discrepancy by $1/2$ between the spectral index k of m_{kr} and the actual frequency $k + 1/2$ of the cosine. We now construct another MLT, where we exchange positions of the symmetry and anti-symmetry constraint in each basis function, i.e. the anti-symmetry constraint is now positioned at $(M-1)/2$, and the symmetry constraint at $(3M-1)/2$. This transform — denoted MLT′ — corresponds to a time-inverted MLT, and is described by a $(M, 2M)$-matrix with entries

$$\begin{aligned} m'_{kr} &= \cos\left[\frac{\pi}{2M}\left(r - M + \frac{1}{2}\right)\right] \cdot \\ &\quad \cdot \sin\left[\frac{\pi}{M}\left(r - \frac{M-1}{2}\right)\left(k + \frac{1}{2}\right)\right], \\ &\quad k = 0, \ldots, M-1,\ r = 0, \ldots, 2M-1. \end{aligned} \tag{2}$$

When processing images, 2D localised spectra can be obtained by performing either MLT or MLT′ in both directions. The central idea of our new transform is to compute both MLT and MLT′, and to obtain new spectra from the sum and the difference of these (Fig. 1). We will show that taken together, these spectra allow to distinguish between mirrored orientations, and hence unambiguous orientation detection.

For each block of $2M \times 2M$ pixels of an image with samples x_{rs} there are $M \times M$ coefficients denoted y_{ij} for the MLT and y'_{ij} for the MLT′. We combine these to LDT coefficients a_{ij} by

$$a_{ij} = \left\{ \begin{array}{l} (y_{i-1/2,j-1/2} - y'_{i-1/2,j-1/2}) \\ (y_{i-1/2,-j-1/2} + y'_{i-1/2,-j-1/2}) \\ a_{-i,-j} \end{array} \right\} \quad \text{if} \quad \left\{ \begin{array}{l} i>0, j>0 \\ i>0, j<0 \\ i<0 \end{array} \right. \quad i,j = -M+\tfrac{1}{2}, \ldots, M-\tfrac{1}{2} \tag{3}$$

Note that, compared to (1), we have here shifted the frequency sampling grid by $1/2$ in each dimension. The indices i, j of a_{ij} do hence correspond again to the spatial frequencies of the sinusoids (see (5)). Moreover, the above defined local spectrum is symmetric with respect to the origin rather than to $(1/2, 1/2)$. Formally, this spectrum consists of $4M^2$ real coefficients, which due to the symmetry result in $2M^2$ independent coefficients. In total, this representation contains twice as many coefficients as the original image.

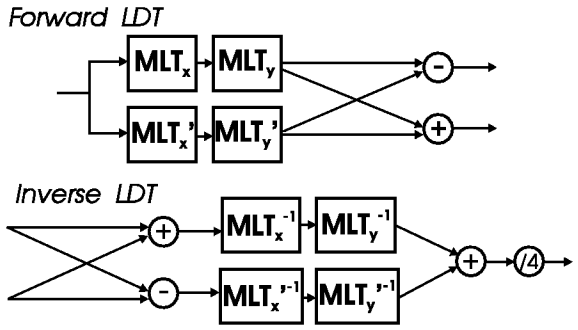

Figure 1: Block diagram of the LDT and its inverse.

A closer look at the LDT's basis functions reveals its ability to identify orientation. Writing the inner product to calculate the LDT coefficients as the sum

$$a_{ij} = \sum_{r,s=0}^{2M-1} d_{ij,rs}\, x_{rs} \tag{4}$$

we obtain for $i, j > 0$

$$\begin{aligned} d_{ij,rs} &= m_{i-1/2,r} m_{j-1/2,s} - m'_{i-1/2,r} m'_{j-1/2,s} \\ &= \cos\left[\frac{\pi}{2M}\left(r - M + \frac{1}{2}\right)\right] \cos\left[\frac{\pi}{2M}\left(s - M + \frac{1}{2}\right)\right] \\ &\quad \left\{\cos\left[\frac{\pi}{M} i \left(r - \frac{M-1}{2}\right)\right] \cos\left[\frac{\pi}{M} j \left(s - \frac{M-1}{2}\right)\right]\right. \\ &\quad \left. - \sin\left[\frac{\pi}{M} i \left(r - \frac{M-1}{2}\right)\right] \sin\left[\frac{\pi}{M} j \left(s - \frac{M-1}{2}\right)\right]\right\} \\ &= \cos\left[\frac{\pi}{2M}\left(r - M + \frac{1}{2}\right)\right] \cos\left[\frac{\pi}{2M}\left(s - M + \frac{1}{2}\right)\right] \\ &\quad \cos\left[\frac{\pi}{M}\left(i(r - \frac{M-1}{2}) + j(s - \frac{M-1}{2})\right)\right], \end{aligned} \tag{5}$$

which is a modulated cosine wave of 2D frequency (i, j). A similar relation holds for $i > 0, j < 0$. These directional basis functions are shown in Fig. 2 in comparison to their non-directional counterparts from the MLT and MLT′. Unlike the MLT and MLT′ basis functions, the 2D LDT basis functions are not separable into real-valued 1D basis functions. On the other hand, the LDT modulus spectrum clearly

distinguishes between mirrored orientations, which neither MLT nor MLT′ do. The LDT's non-separability is no serious drawback, since it is calculated from two separable transforms.

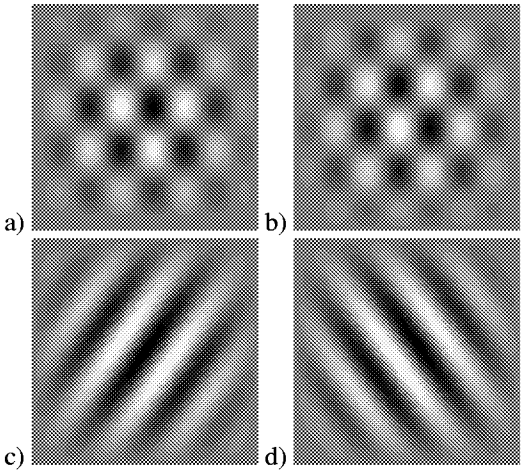

Figure 2: Example 2D MLT and LDT basis functions: a) basis function for coefficient $(3, 2)$ of the MLT, b) of the MLT′, c) LDT basis function $(3.5, 2.5)$, d) LDT basis function $(3.5, -2.5)$.

The LDT can easily be inverted since both MLT and MLT′ coefficients can be recovered from the LDT coefficients as follows:

$$y_{kl} = \frac{1}{2}(a_{k+1/2,l+1/2} + a_{k+1/2,-l-1/2}) \quad (6)$$

$$y'_{kl} = \frac{1}{2}(-a_{k+1/2,l+1/2} + a_{k+1/2,-l-1/2}) \quad (7)$$

In theory, one of these data sets — y_{kl} or y'_{kl} — suffices for perfect image reconstruction. In practice, however, both spectra will be processed. In order to reconstruct the processed image with respect to the oriented basis functions, we therefore calculate both the inverse MLT and inverse MLT′, and take the average of these. This is also illustrated in Fig. 1.

3. APPLICATION TO IMAGE RESTORATION

We have applied the LDT within the algorithm for noise reduction and enhancement of low dose X-ray images described in [4]. The algorithm's block diagram is depicted in Fig. 3. The input image is first decomposed into local spectra, where the DFT was used in [4]. Each spectral coefficient is then related to its noise variance by calculating the (instantaneous) signal to noise ratio (S/N), where in [4] the noise variance in the spectral domain is obtained from calibration measurements of the noise power spectrum of the given imaging system, and stored in the noise model box. Coefficients with low S/N are then attenuated, with the relation between attenuation and S/N being captured by a noise attenuation curve (cf. Fig. 4). In our experience, this approach — termed spectral amplitude estimation — is particularly well suited to low dose X-ray images where noise is coloured [3].

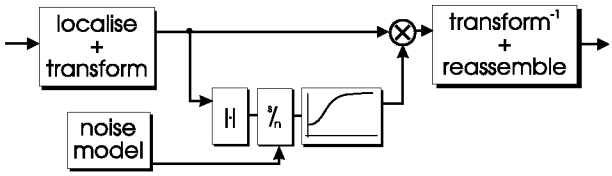

Figure 3: Overview of noise reduction using spectral amplitude estimation.

The key feature of the algorithm in [4] is its adaptivity to local orientation. To this end, each local spectrum is analyzed by means of an *inertia matrix* to identify the line along which spectral energy concentration is strongest. Since the DFT is used, this line is unambiguously related to an oriented structure in the spatial domain, like lines or edges.

With σ_{ij}^2 denoting the noise variance for DFT coefficient g_{ij}, the inertia matrix is given by

$$\begin{pmatrix} \sum_{i,j} \frac{i^2}{i^2+j^2} \frac{|g_{ij}|^2}{\sigma_{ij}^2} & \sum_{i,j} \frac{ij}{i^2+j^2} \frac{|g_{ij}|^2}{\sigma_{ij}^2} \\ \sum_{i,j} \frac{ij}{i^2+j^2} \frac{|g_{ij}|^2}{\sigma_{ij}^2} & \sum_{i,j} \frac{j^2}{i^2+j^2} \frac{|g_{ij}|^2}{\sigma_{ij}^2} \end{pmatrix} \quad (8)$$

If the block contains a dominant structure the two eigenvalues of this matrix differ strongly. The eigenvector belonging to the smaller eigenvalue determines the line with strongest energy concentration. In [4], this information is used to modulate the attenuation depending on the processed coefficient's position relative to the orientation axis. Assuming that spectral coefficients along or close to the orientation axis contribute to perceptually important detail, less attenuation is applied to these for any given S/N. This is depicted in Fig. 4. In [4], we used the orientation information even to selectively enhance these coefficients.

The LDT can be used within this approach in the same manner as the DFT. As the LDT behaves like the DFT with respect to local orientation, the algorithm's ability to preserve or even emphasize visually important structures remains untouched.

An example of a low dose X-ray image is given in Fig. 5. An enlarged portion of this image is shown in Fig. 6 side by side to its processed version. A comparison between these reveals that noise was indeed appreciably suppressed, while the guidewire was visibly enhanced. Qualitative and quantitative comparisons showed that the LDT performs as well as the DFT within this algorithm. The DFT-based algorithm, however, was redundant by a factor of four, whereas the LDT-based algorithm is redundant by a factor of only two.

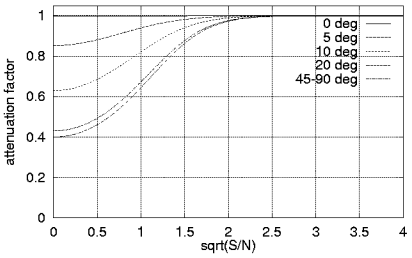

Figure 4: Attenuation curves used for noise reduction. The attenuation factor is shown as a function of the ratio of coefficient magnitude and noise standard deviation (cf. Fig. 3). Depending on the angle of a coefficient's position relative to the dominant orientation the attenuation is reduced.

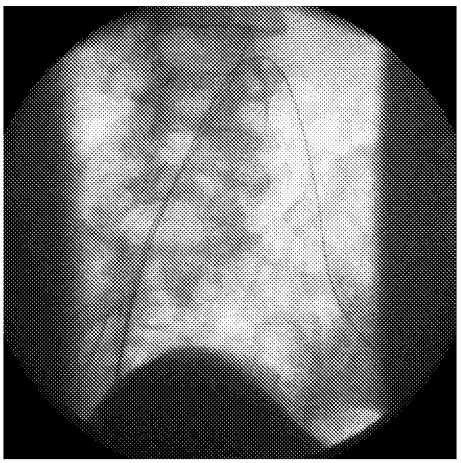

Figure 5: A low dose X-ray image depicting a guidewire within a patient's vascular system.

4. CONCLUSION

We have derived a new real-valued transform referred to as LDT with inherently overlapping basis functions. Unlike other real-valued standard transforms like the DCT or MLT, the new transform uses directional basis functions like the complex-valued DFT, hence providing for an unambiguous relationship between orientation in the spatial domain and concentration of energy in the spectral domain. We have furthermore described an anisotropic spectral magnitude estimation algorithm for image restoration where this orientation property was exploited to improve performance with respect to perceptually relevant detail. Both DFT-based and LDT-based versions of this algorithm perform comparably, with the LDT generating less redundancy than the DFT. Although the LDT's basis functions are not separable, it is calculated invoking a separable transform, viz. the MLT. Since fast algorithms exist for the MLT [8], so do fast algorithms for the LDT.

LDT and DFT differ in the grid on which the frequencies are sampled. Whereas DFT refers to an integer grid, the

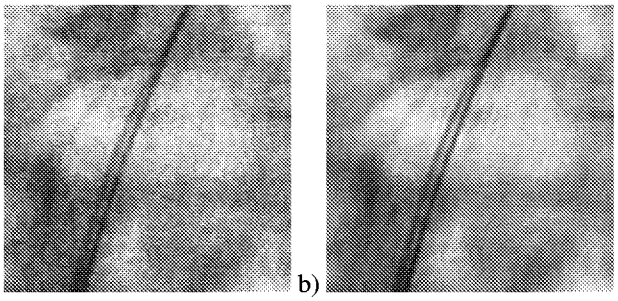

Figure 6: Zoomed section of the X-ray image in Fig. 5: a) original, b) processed by LDT-based anisotropic spectral magnitude estimation.

LDT grid is shifted by $1/2$ in both directions. This implies that there is neither a coefficient for 0 nor for the Nyquist frequency which makes handling of the data easier.

A more basic question is whether a non-redundant alternative to the LDT exists, i.e. a real-valued lapped transform with fast algorithm, no redundancy, and an unambiguous representation of orientation. As long as such a transform is not known, further study of the LDT is worth its effort.

5. REFERENCES

[1] R. J. Clarke, *Transform Coding of Images*. London: Academic Press, 1985.

[2] J. S. Lim, "Image restoration by short space spectral subtraction," *IEEE T ASSP* 28(2), 191–197, 1980.

[3] T. Aach, D. Kunz, "Spectral estimation filters for noise reduction in x-ray fluoroscopy imaging," *Proc. EUSIPCO-96* (G. Ramponi et.al, eds.), Edizioni LINT, Trieste, 571–574, 1996.

[4] T. Aach, D. Kunz, "Anisotropic spectral magnitude estimation filters for noise reduction and image enhancement," *Proc. IEEE ICIP*, Lausanne, 335–338, 1996.

[5] J. Bigün, G. H. Granlund, "Optimal orientation detection of linear symmetry," *Proc. IEEE 1. ICCV*, London, 433–438, 1987.

[6] R. E. Crochiere, "A weighted overlap-add method of short-time Fourier analysis/synthesis," *IEEE T ASSP* 28(1), 99–102, 1980.

[7] H. S. Malvar, D. H. Staelin, "The LOT: Transform coding without blocking effects," *IEEE T ASSP* 37(4), 553–559, 1989.

[8] H. S. Malvar, "Lapped transforms for efficient transform/subband coding," *IEEE T ASSP* 38(6), 969–978, 1990.

[9] M. Breeuwer, R. Heusdens, P. Zwart, "Overlapped transform coding of medical x-ray images," SPIE Vol. 2164, 1994.

[10] R. W. Young, N. G. Kingsbury, "Frequency-domain motion estimation using a complex lapped transform," *IEEE T IP* 2(1), 2–17, 1993.